Journal of Power Sources 244 (2013) 300–305

Contents lists available at SciVerse ScienceDirect

Journal of Power Sources

journal homepage: www.elsevier.com/locate/jpowsour

Cr and V substituted $LiSn_2P_3O_{12}$ solid electrolyte materials

R. Norhaniza [a,*], R.H.Y. Subban [b], N.S. Mohamed [c]

[a] Institute of Graduate Studies, University of Malaya, 50603 Kuala Lumpur, Malaysia
[b] Faculty of Applied Sciences, Universiti Teknologi MARA, 40450 Shah Alam, Selangor, Malaysia
[c] Center for Foundation Studies in Science, University of Malaya, 50603 Kuala Lumpur, Malaysia

HIGHLIGHTS

- $Li_{1.8}Cr_{0.8}Sn_{1.8}P_{3-y}V_yO_{12}$ pellets were obtained without using any binding agent.
- V substitution enhances bulk conductivity of $LiSn_2P_3O_{12}$ by two orders of magnitude.
- V substitution increases grain boundary conductivity by one order of magnitude.
- Conductivities changes are attributed to structural changes due to V substitution.

ARTICLE INFO

Article history:
Received 22 October 2012
Received in revised form
17 December 2012
Accepted 29 December 2012
Available online 16 January 2013

Keywords:
Crystallinity
Lithium ion conductor
Nasicon
Mechanical milling

ABSTRACT

$Li_{1+x}Cr_xSn_{2-x}P_{3-y}V_yO_{12}$ solid electrolyte materials with $x = 0.8$ and $y = 0$, 0.2, 0.4, 0.6 and 0.8 are prepared by mechanochemical milling method followed by heat treatment at 1000 °C. The conductivities of the pellets are determined using AC impedance spectroscopy. X-ray diffraction is used to determine the crystallographic phases while scanning electron microscope and energy dispersive X-ray are used to study morphological properties and elemental compositions respectively. Combined substitution of both chromium and vanadium in $LiSn_2P_3O_{12}$ system results in enhancement of room temperature ionic conductivity up to two orders of magnitude compared to the unsubstituted $LiSn_2P_3O_{12}$ system. The increase in conductivity in the systems with y of 0.2 and 0.4 as compared to the sample of $y = 0$ is attributed to the absence of $Li_6P_6O_{18}$ impurities. Furthermore, the sample with $y = 0.4$ shows higher ionic conductivity compared to the sample with $y = 0.2$. This sample exhibits bulk conductivity of 10^{-3} S cm^{-1} and grain boundary conductivity of 10^{-5} S cm^{-1} at elevated temperatures. This is attributed to larger crystallite size and better contact between grains. This sample is also structurally stable toward temperature and thus suitable for thermal electrochemical device application.

1. Introduction

Sodium superionic conductors, which are also known as NASICON has a structure with 3D back-bone skeleton, were first discovered by Goodenough et al. [1]. This structure favors high ionic conductivity at high temperature due to mobile sodium ions [2,3]. Lithium analogous NASICON has the same structure but with lithium (Li^+) ions as the mobile species. This type of materials has been reported in various papers [4–8]. Most works reported in the literature are on Ge, Hf, Ti and Zr containing systems. $LiSn_2P_3O_{12}$ (LSP) also possesses NASICON type structure [8,9]. Juarez et al. [9] and Lazarraga et al. [10] have reported conductivity behavior of this material. The studies were done by mixing teflon with $LiSn_2P_3O_{12}$. Teflon was used as a binder to improve the stability of $LiSn_2P_3O_{12}$ pellets since the sintered $LiSn_2P_3O_{12}$ pellets were fragile for handling and easily broken due to phase change phenomenon [10,11]. However, the pellets showed low conductivity (10^{-10} S cm^{-1}) at room temperature. Previously the authors of this article have succeeded in obtaining stable $LiSn_2P_3O_{12}$ pellets without employing any binder using the technique of mechanical milling [12]. The pellets exhibited conductivity values in the order of 10^{-7} S cm^{-1} at room temperature. The authors have observed a conductivity increase for pellets of V substituted $LiSn_2P_3O_{12}$ pellets [13].

In this work, the $LiSn_2P_3O_{12}$ compound was substituted with both Cr^{3+} and V^{5+} at Sn^{4+} and P^{5+} site respectively in order to further improve its conductivity. The expected general formula of this partially substituted system is $Li_{1+x}Cr_xSn_{2-x}P_{3-y}V_yO_{12}$. In the work of Cr substituted $LiSn_2P_3O_{12}$ done earlier [14], the authors obtained the highest room temperature conductivity value of

* Corresponding author. Tel.: +60 379675972; fax: +60 379576478.
E-mail address: r.norhaniza@ymail.com (R. Norhaniza).

0378-7753/$ – see front matter © 2013 Elsevier B.V. All rights reserved.
http://dx.doi.org/10.1016/j.jpowsour.2012.12.119

10^{-6} S cm^{-1} for $Li_{1.8}Cr_{0.8}Sn_{1.2}P_3O_{12}$ system. In the present system, the value of Cr content was fixed at $x = 0.8$ while the value of V content (y) was varied. Substitutions of V^{5+} at P^{5+} sites form $(VO_4)^{3-}$ tetrahedra which are larger than $(PO_4)^{3-}$ tetrahedra are expected to enlarge bottlenecks which are the conducting channels leading to increase in mobility of Li^+ ions and hence enhancing conductivity [1,4–8].

2. Experimental

In this work, the chemicals used were Li_2O 99% (Aldrich), SnO_2 98% (Aldrich), $NH_4H_2PO_4$ 98% (Aldrich), V_2O_5 98% (Aldrich) and Cr_2O_3 99%. Stoichiometric mixtures of the starting materials were pre-heated in crucibles at 700 °C for 2 h. The pre-heating process was done to decompose NH_4 and H_2O from $NH_4H_2PO_4$ to obtain P_2O_5 [10,15]. The resultant mixtures were put together with zirconium (Zr) balls in a bowl for mechanochemical milling process. Milling process was done using Fristch 7 ball mill for 80 h. The milled mixtures were then pelletized under a pressure of 7 ton using Specac Hydraulic Press to form pellets with diameter and thickness of 13 mm and 1–2 mm respectively [13]. The pellets were then sintered at temperatures between 700 and 1000 °C for 8 h. This process was done to determine the optimum sintering temperature for obtaining optimum conductivity. It was observed that for each y value, the highest conductivity was obtained at sintering temperature of 1000 °C. For further analysis, samples were prepared by sintering them at their optimized sintering temperature and they were labeled as CV0, CV2, CV4, CV6 and CV8 according to their value of y of 0, 0.2, 0.4, 0.6 and 0.8 respectively. The sintered pellets were kept in desiccators before characterization were carried out.

The prepared samples were subjected to various studies. Structural properties of the samples were studied using Bruker AXS D8 Advance X-ray Diffraction spectrometer with Cu-K_α radiation of wavelength of 1.5406 Å in 2θ range between 3° and 90°. The structures of $Li_{1.8}Cr_{0.8}Sn_{1.8}P_{3-y}V_yO_{12}$ as a function of y were determined using the R-3c structure of $LiSn_2P_3O_{12}$ as a starting material. The refinements were done by using Xpert XRD software. Conductivity of the pellets was determined by impedance spectroscopy using Solartron SI 1260 Impedance Analyzer in the frequency range from 32 MHz to 1 Hz. For each y value, average conductivity value was calculated using the data obtained for six samples. The surface morphology images of the samples were examined using FEI Quanta 200 FESEM. The samples were examined under a vacuum condition with magnification of 200 000× and accelerating voltage of 20 kV. Elemental analyses of the samples were done using energy dispersive X-ray (EDX) in conjunction with scanning electron

Table 1
Lattice parameter of $Li_{1.8}Cr_{0.8}Sn_{1.2}P_{3-y}V_yO_{12}$.

Sample	a (Å)	b (Å)	c (Å)	V (Å^3)
CV0	8.351	8.351	22.370	1351.00
CV2	8.358	8.355	22.380	1353.83
CV4	8.411	8.359	19.029	1349.07
CV6	8.617	8.361	16.567	1093.00
CV8	8.694	8.033	11.952	805.25

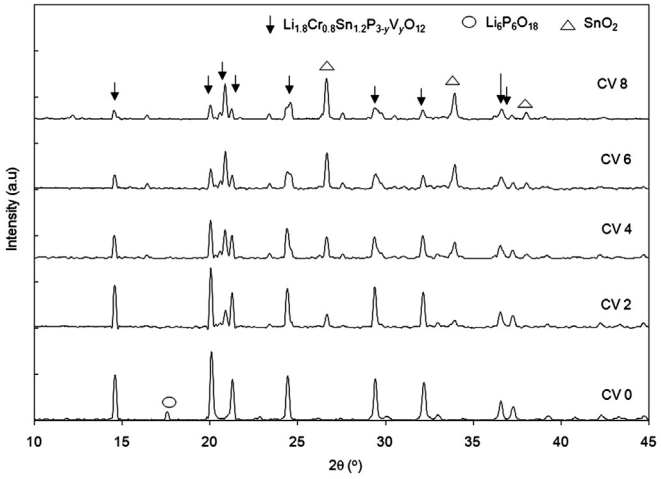

Fig. 1. X-ray diffraction patterns of CV0, CV2, CV4, CV6 and CV8.

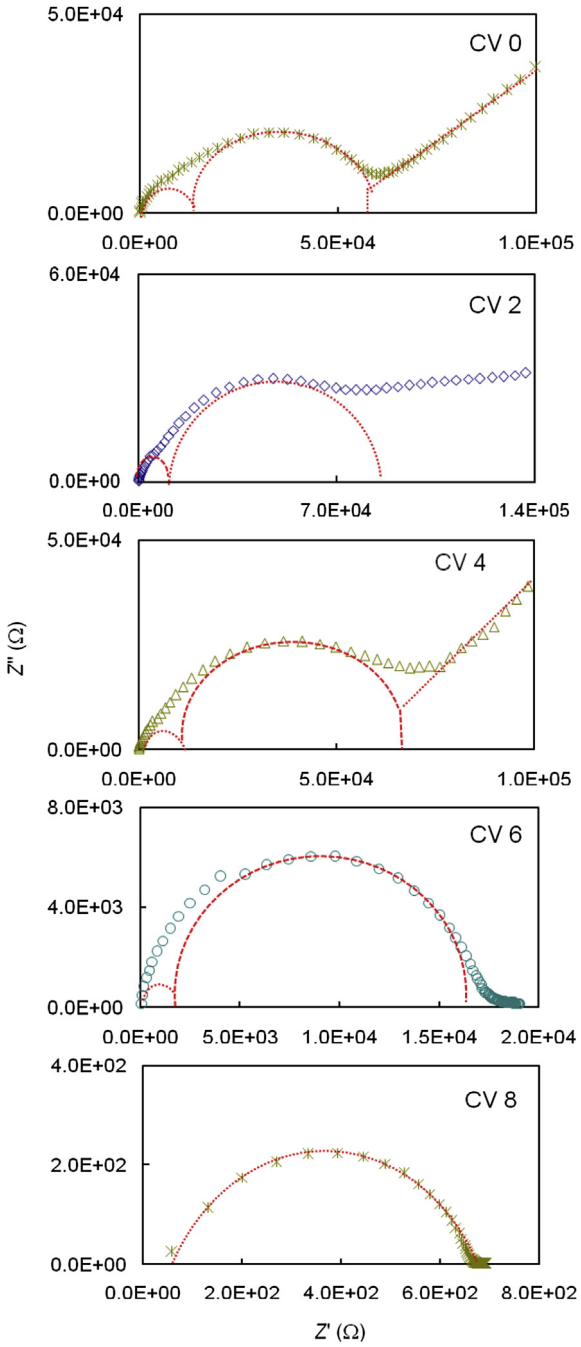

Fig. 2. Typical impedance plot of CV0, CV2, CV4, CV6 and CV8.

microscope (SEM). Ionic transference number was analyzed by Wagner's polarization and carbon was used as the blocking electrodes. In order to determine the actual type of charge carriers, Li^+ ion transference number measurement was done using a combination of AC impedance spectroscopy and DC polarization technique. For this measurement, lithium metal was used as the non-blocking electrodes. All measurements were done on Solartron SI 1260 Impedance Analyzer with SI 1287 Electrochemical Interface in an argon filled glove box with $O_2 < 0.1$ ppm and $H_2O < 0.1$ ppm.

3. Results and discussion

Fig. 1 shows the XRD spectra of the studied samples. The spectrum of CV0 is characterized by the presence of $Li_6P_6O_{18}$ and SnO_2 impurities. Only SnO_2 is observed in CV2, CV4, CV6 and CV8. This suggests that addition of vanadium eliminated the formation of $Li_6P_6O_{18}$ impurity. The absence of peaks attributed to any chromium and vanadium related compound in the XRD spectra suggests that partial substitution has taken place. Table 1 shows refinement of the lattice parameter. The Cr substituted sample (CV0) has smaller *a*-parameter compared to LSP. Addition of V shows an increase in the *a*-parameter. Both CV0 and CV2 exhibit rhombohedral structure while CV4, CV6 and CV8 have a monoclinic structure. All samples still remain their NASICON structure. It is also observed that CV0, CV2 and CV4 have a similar volume cell while in CV6 and CV8, there is a decrease in the cell volume. The changes in lattice parameters can be attributed to the ionic radius difference where $Sn^{4+} = 0.65$ Å, $Cr^{3+} = 0.62$ Å, $P^{5+} = 0.17$ Å and $V^{5+} = 0.36$ Å. In the substitution of Sn^{4+} by Cr^{3+}, which is smaller than Sn^{4+} there is a small decrease in the *a* parameter and the decrease of the *b* and *c* parameter. The addition of Cr^{3+} ions simultaneously produced additional Li^+ ions in order to balance the charge in the structure. Thus the adjustment in lattice parameters is due to accommodation of the structure to occupy

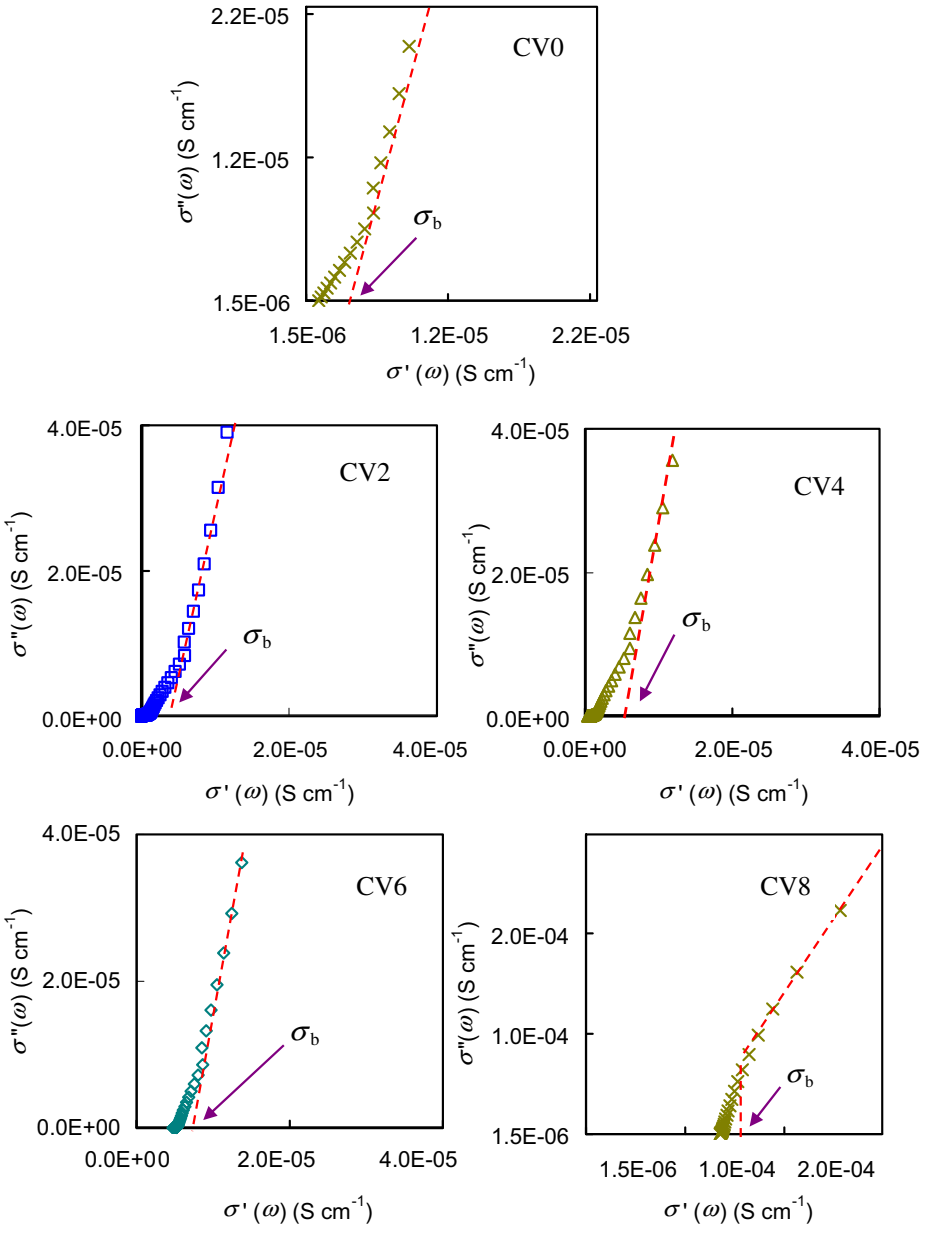

Fig. 3. Conductivity plots of CV0, CV2, CV4, CV6 and CV8.

the extra Li^+ ion [3]. The expansion in *a* parameter due to addition of V is also resulted from accommodation of structure with partial substitution ion. The larger radii of V^{5+} causes the expansion of the framework along *a*-direction and a concomitant contraction in structure along the *c*-direction [1,3].

Fig. 2 shows typical complex impedance plots for all samples. In the case of CV0, CV2 and CV4, the plots seem to consist of two overlapping semicircles with a spike at low frequency region. However, for CV6, only overlapping semicircles are observed without the presence of a spike. For CV8, only one semicircle is present. Since all semicircles overlap each other it is difficult to determine the value of R_g and R_{gb} from the complex impedance plots. As an alternative the values of σ_b was determined by plotting imaginary part of conductivity, σ'' versus real part of conductivity, σ' plots. The same technique has been used by other researchers [16–19]. The conductivity spectra for all samples studied in this work are illustrated in Fig. 3. The conductivity plots consisted of a semicircle and two dispersion curves at medium σ' and high σ' regions. The conductivity variations with *y* are presented in Fig. 4. Both σ_b and σ_{gb} increase with increase in *y* content. All samples show conductivity enhancement of about an order of magnitude except for CV8, which shows an enhancement of two orders of magnitude when compared to CV0.

All the samples were subjected to ionic transference number measurement using DC polarization technique. Fig. 5 presents the DC polarization curves for all samples. The calculated values of the ionic transference numbers are 0.99, 0.97, 0.95, 0.55 and 0.49 for CV0, CV2, CV4, CV6 and CV8 respectively. Since the values of transference numbers for samples CV0, CV2, and CV4 are close to unity, it is inferred that they are ionic conductors. CV6 and CV8 are considered as mixed ionic–electronic conductors as their transference numbers are about 0.5. High electronic contribution to conductivity in CV6 and CV8 is due to the presence of SnO_2 in significant amount in these systems [20].

Since the interest of this study is on ionic conducting solid electrolytes, lithium transference number measurement was only carried out on CV2 and CV4 in order to ascertain the type of conducting species. For this purpose, the samples were sandwiched between lithium metal electrodes. Fig. 6 shows the impedance plots while Fig. 7 illustrates the normalized current–time plot for both CV2 and CV4. Both impedance plots consist of two semicircles with intercepts at Z' axis which corresponded to R_b and R_e (R_e is secondary passive layer resistance). The values of Li ion transference number, τ_{Li}^{+} was calculated using equation obtained from Refs. [21,22]. Table 2 lists the values of R_b, R_e, I_∞ and τ_{Li}^{+} obtained from this measurement. The values of τ_{Li}^{+} are 0.86 and 0.90 for CV2 and CV4 respectively. These values indicate that the majority charge carriers in the samples are Li^+ ions.

As mentioned earlier, CV4 exhibits conductivity of an order of magnitude higher than CV0. This is ascribed to absence of $Li_6P_6O_{18}$

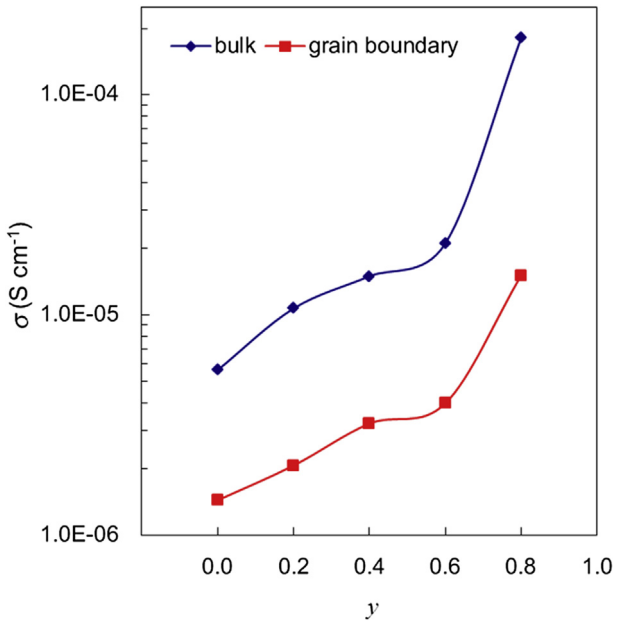

Fig. 4. Conductivity variation with *y*.

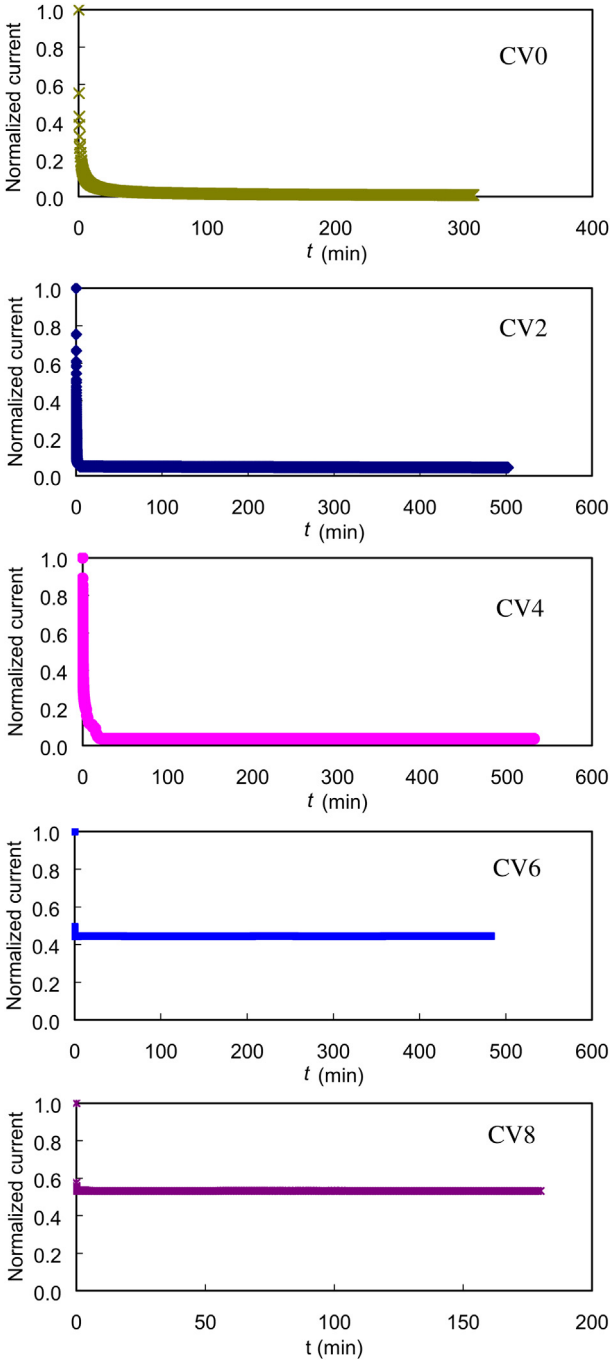

Fig. 5. Normalized current versus time of CV0, CV2, CV4, CV6 and CV8 (measurements were done using carbon blocking electrodes).

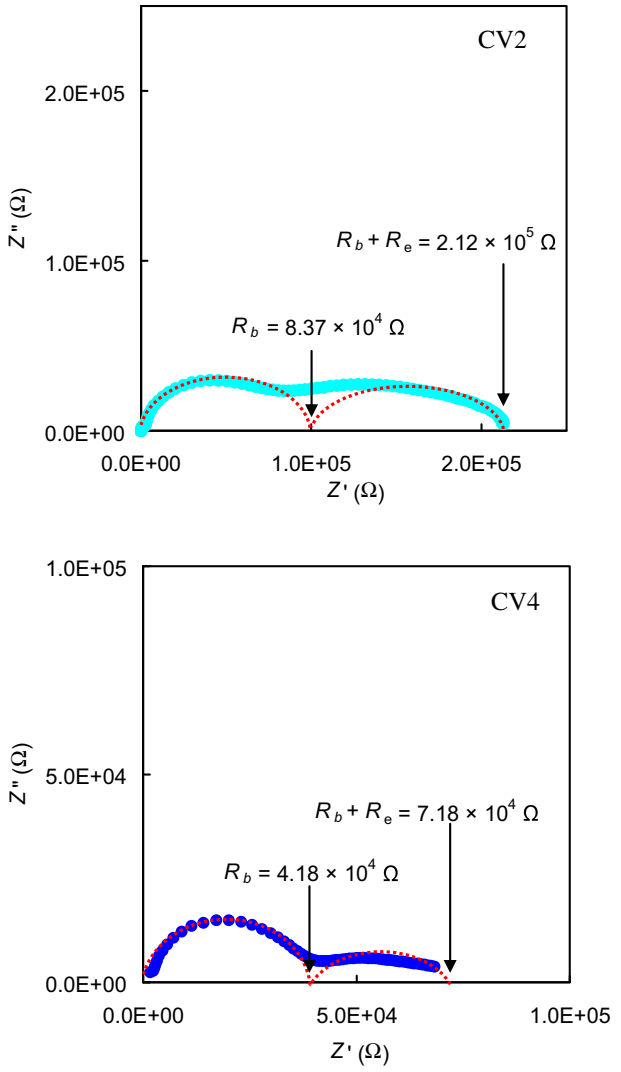

Fig. 6. Impedance plots of CV2 and CV4 (measurements were done using lithium non-blocking electrodes).

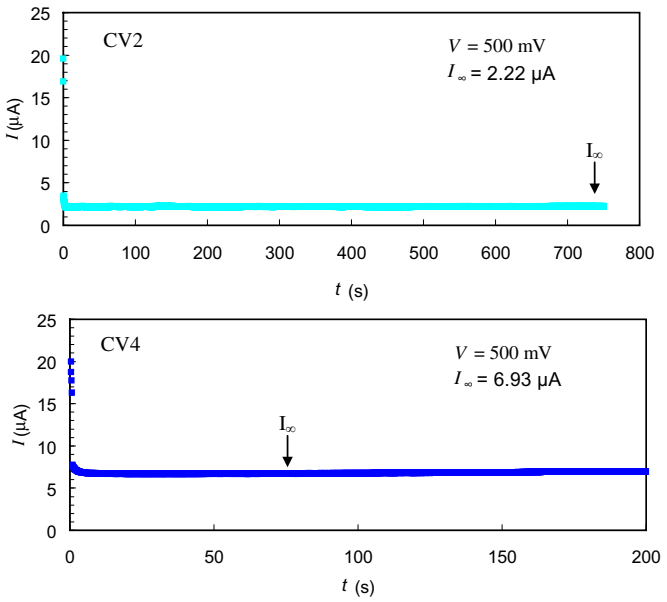

Fig. 7. Normalized current versus time of CV2 and CV4 (measurements were done using lithium non-blocking electrodes).

impurities. The absence of $Li_6P_6O_{18}$ impurities led to easy migration of Li^+ ions between grains [23,24]. Furthermore, CV4 shows higher conductivity than CV2. Crystallite measurement reveals that CV4 has greater crystallites compared to CV2. The average crystallite size for CV2 is 358.66 ± 0.01 Å and for CV4 is 376.20 ± 0.01 Å. Thus the higher value of conductivity for CV4 could be attributed to greater crystalline phase which is the conducting phase in the systems. According to Fu [25], the enhancement in crystalline phase favors high ion conduction due to the presence of larger conduction pathways for Li^+ ions migration. A similar observation has been reported by Chowdari et al. [26]. The change in lattice parameter can also contribute to conductivity enhancement since it changes the bottleneck size and results in easy mobility of ion [27].

SEM was also performed on CV2 and CV4 and their micrographs are shown in Fig. 8 for comparison purpose, SEM micrograph of CV0 is also presented in this figure. It is obvious that there is change in morphology from granular structure in CV0 system into cubic structure in CV2 and CV4. Similar observation was observed by Chang et al. [27] when V was substituted in $Li_{1+x}Al_xTi_{2-x}P_3O_{12}$. Furthermore, the grains in CV4 are larger compared to those in CV2. According to Aono et al. [28], increase in cubic size indicates an increase in density of the samples resulting in an increase in conductivity. The increase in size of cubic structure also leads to a decrease in the number of grain boundaries resulting in a decrease in grain boundary resistance and improve the grain boundary conductivity value. This is another factor of why CV4 has higher conductivity than CV2.

In order to confirm that substitution has taken place, EDX analysis was done on CV2 and CV4. Elemental compositions from EDX analysis are listed in Table 3. In CV2, the ratio of Cr:Sn:P:V is equivalent to the stoichiometric formula 0.8:1.2:2.8:0.2. Since Li^+ ion was not detectable by EDX, the concept of charge neutrality was employed [29–31]. Using this concept, it is inferred that the ratio of Li:Cr:Sn:P:V in the compound was 1.8:0.8:1.2:2.8:0.2 confirming that the compound synthesized is $Li_{1.8}Cr_{0.8}Sn_{1.2}P_{2.8}V_{0.2}O_{12}$. The atomic ratio of elements in CV4 is also similar to the atomic ratios of the starting materials. This confirms that chromium and vanadium have been successfully substituted into Sn and P sites in $LiSn_2P_3O_{12}$ matrix.

Analysis on temperature dependence of conductivity behavior was carried out on CV4. This behavior is shown in Fig. 9. As observed in this figure, CV4 presents a linear σ–T plot indicating that there was no phase transition. This implies that this system is structurally stable toward temperature in the studied temperature range. The increase in conductivity with temperature is attributed to an increase in vibration of ions with increase in temperature leading to formation of free ions and enhancement in conductivity. This sample also shows low value of bulk activation energy, $E_{a,b}$ and grain boundary activation energy, $E_{a,gb}$ of 0.09 eV and 0.40 eV respectively suggesting high mobility of ions.

Table 2
Data obtained from Li^+ transference number measurement.

Sample	R_b (±0.01 Ω)	R_e (±0.01 Ω)	I_∞ (±0.01 μA)	τ_{Li}^+ (±0.01)
CV2	8.37×10^4	1.28×10^5	2.22	0.86
CV4	4.18×10^4	3.00×10^4	6.93	0.90

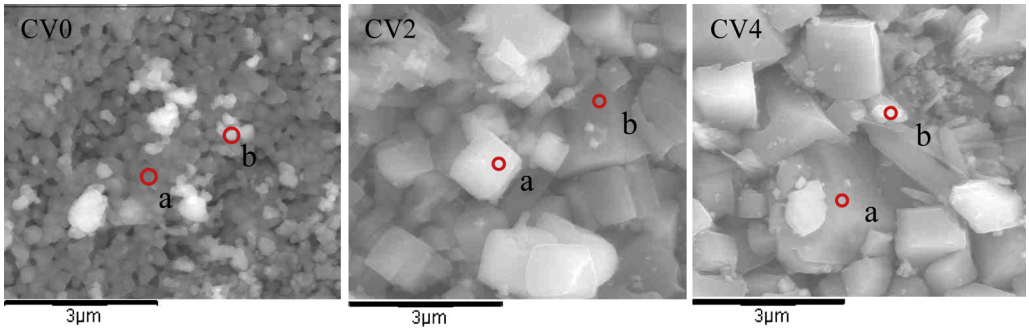

Fig. 8. SEM image of CV0, CV2 and CV4.

Table 3
Atomic percentage of elements at points a and b from SEM image for CV0, CV2 and CV4.

Sample	Composition	Atomic percentage				Stoichiometric ratio Cr:Sn:P:V
		Cr	Sn	P	V	
CV0	Starting mixture	16.00	24.00	60.00	0	0.8:1.2:3.0:0
	CV0 – a	15.45	23.66	60.89	0	0.76:1.17:3.00:0
	CV0 – b	15.86	23.71	60.43	0	0.79:1.18:3.00:0
CV2	Starting mixture	15.98	24.01	56.01	4	0.8:1.2:2.8:0.2
	CV2 – a	15.8	23.82	56.38	4.00	0.78:1.18:2.8:0.19
	CV2 – b	16.61	23.63	56.00	3.76	0.84:1.20:2.84:0.19
CV4	Starting mixture	15.98	24.00	52.00	8.02	0.8:1.2:2.6:0.4
	CV4 – a	15.82	23.84	52.21	8.13	0.79:1.19:2.6:0.40
	CV4 – b	15.87	23.80	53.13	7.20	0.78:1.16:2.6:0.35

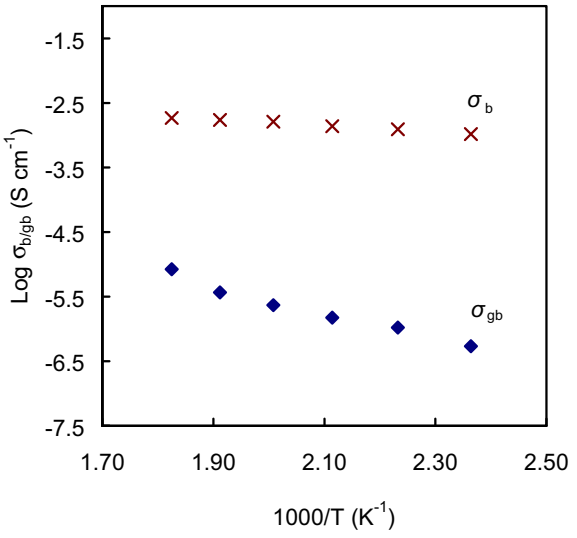

Fig. 9. Temperature dependence of conductivity for CV4.

4. Conclusion

Combined substitution of Cr and V in $LiSn_2P_3O_{12}$ system enhances the room temperature ionic conductivity by one order of magnitude compared to the Cr substituted $LiSn_2P_3O_{12}$ system and two orders of magnitude compared to the unsubstituted $LiSn_2P_3O_{12}$. The samples with $y = 0.2$ and 0.4 are lithium ion conductors as indicated by their lithium ion transference number. The sample with $y = 0.4$ shows the highest conductivity of the order of 10^{-5} S cm^{-1} at room temperature and 10^{-3} S cm^{-1} in temperature range from 150 to 275 °C. This sample also did not show any phase transition in the temperature range studied in this work and thus possibly applicable as electrolyte in thermal electrochemical devices.

References

[1] J.B. Goodenough, H.Y.P. Hong, J.A. Kafalas, Material Research Bulletin 11 (1976) 203–220.
[2] P. Yadav, M.C. Bhatnagar, Ceramic International 38 (2012) 1731–1735.
[3] F.J. Berry, N. Costantini, L.E. Smart, Solid State Ionics 177 (2006) 2889–2896.
[4] J. Sanz, J.M. Rojo, R. Jimenez, J.E. Inglesias, Solid State Ionics 62 (1993) 287–292.
[5] W. Wang, J. Chen, J. Zhao, Solid State Ionics: Material and Application (1992) 369–372.
[6] J. Wolfenstine, J.L. Allen, J. Summer, J. Sakamoto, Solid State Ionics 180 (2009) 961–967.
[7] M.A. Paris, A.M. Juarez, J.M. Rojo, J. Sanz, Journal Physical Condensed Materials 8 (1996) 5355–5366.
[8] A.D. Robertson, A.R. West, A.G. Ritchie, Solid State Ionics 104 (1997) 1–11.
[9] A.M. Juarez, R. Jimenez, P.D. Martin, J. Ibanez, J.M. Rojo, Journal Physics: Condensed Matter 9 (1997) 4119–4128.
[10] M.G. Lazarraga, J. Ibañez, M. Tabellout, J.M. Rojo, Composites Science and Technology 64 (2004) 759–765.
[11] J.M. Winand, A. Rulmont, P. Tarte, Journal of Solid State Chemistry 93 (1991) 341–349.
[12] R. Norhaniza, R.H.Y. Subban, N.S. Mohamed, Advanced Materials Research 129-131 (2010) 338–342.
[13] R. Norhaniza, R.H.Y. Subban, N.S. Mohamed, Journal Materials Science 46 (2011) 7815–7821.
[14] R. Norhaniza, R.H.Y. Subban, N.S. Mohamed, A. Ahmad, International Journal Electrochemical Science 7 (2012) 10254–10265.
[15] B.J. Ward, C.C. Liu, G.W. Hunter, Journal of Materials Science 21 (2003) 4289–4292.
[16] A.F. Orliukas, A. Dindune, Z. Kanepe, J. Ronis, B. Bagdonas, A. Kezionis, Electrochimica Acta 51 (2006) 6194–6198.
[17] R. Sobiestianskas, A. Dindune, Z. Kanepe, J. Ronis, A. Kezionis, E. Kazakevicius, A. Orliukas, Materials Science and Engineering B 76 (2000) 184.
[18] M. Cretin, P. Fabry, Journal European Ceramic Society 19 (1999) 2931.
[19] M. Godickemeier, B. Michel, A. Orliukas, P. Bohac, K. Sasaki, L. Gauckler, H. Heinrich, P. Schwander, G. Kostorz, H. Hofmann, O. Frei, Journal Materials Research 9 (1994) 1228–1240.
[20] P. Jozwiak, J.E. Garbarczyk, Solid State Ionics 176 (2005) 2163–2166.
[21] K.S. Sidhu, S.S. Sekhon, S.A. Hashmi, S. Chandra, Journal of Materials Science Letters 12 (1993) 346–349.
[22] S.S. Sekhon, G. Singh, S.A. Angihorty, S. Chandra, Solid State Ionics 80 (1995) 37–44.
[23] A. Mei, Q.H. Jiang, Y.H. Lin, C.W. Nan, Journal of Alloys and Compounds 486 (2009) 871–875.
[24] Q. Zhang, Z. Wen, Y. Liu, S. Song, X. Wu, Journal of Alloys and Compounds 479 (2009) 494–499.
[25] J. Fu, Journal of American Ceramic Society 80 (1997) 1901–1903.
[26] B.V.R. Chowdari, G.V.S. Rao, G.Y.H. Lee, Solid State Ionics 136–137 (2000) 1067–1075.
[27] C.M. Chang, Y.I. Lee, S.H. Hong, Journal of American Ceramic Society 88 (2005) 1803–1807.
[28] H. Aono, E. Sugimoto, Y. Sadaoka, N. Imanaka, G.Y. Adachi, Solid State Ionics 62 (1993) 309–316.
[29] J.L.N. Semanate, A.C.M. Rodrigues, Solid State Ionics 181 (2010) 1197–1204.
[30] F. Wu, Y. Liu, R. Chen, S. Chen, G. Wang, Journal of Power Sources 189 (2009) 467–470.
[31] R. Ramaraghavulu, S. Buddhudu, Ceramic International 37 (2011) 3651–3656.